

Well Productivity of Gas-Condensate Fields : Influence of Connate Water and Condensate Saturation on Inertial Effects

J-M Lombard, D. Longeron & F. Kalaydjian
Institut Français du Pétrole

Abstract

Reliable predictions of productivity decline of gas-condensate wells require a proper description of complex flow behavior occurring in the near wellbore region. In that region, high pressure gradient induces both large condensate saturation and high gas velocities which may lead to significant deviations from Darcy's law for gas permeability. At the present time, no physically relevant model exists which takes into account these non-Darcian two phase flow phenomena.

This paper presents a contribution to the improvement of the description of gas-condensate flowing properties in the near-wellbore region. Specific laboratory equipment has been built in order to perform gas-condensate displacements under conditions as representative as possible of near wellbore conditions. The developed prototype allows gas-condensate displacements under pressure (200 bar) and temperature (120°C) and at velocities up to 1.5 cm/s.

A laboratory study has been performed with the aims (i) to estimate the influence of the pore structure on the gas inertial coefficient β and (ii) to integrate the effect of the condensate dropout in the Forchheimer flow equation.

Experiments were conducted to measure inertial coefficient, β , on sandpicks and sandstone core samples, with and without connate water saturation (S_{wi}), using dry gas (Nitrogen) and analog gas-condensate systems (C1-C3 mixtures).

For dry gas floods, the measured β -values were found in good agreement with previous published data. β -values increase with water (immobile) saturation and a new correlation between β and a mean pore radius, r^* , is proposed.

Prior to conducting gas-condensate floods, 1D numerical simulations were used to optimize the experimental conditions of corefloods with various C1-C3 mixtures i.e., inlet/outlet pressures leading to selected condensate saturations. Experiments performed at different values of condensate saturation show that β -values increase with the total liquid saturation.

Finally, some insights are given for the future work to document more extensively the variation of β -coefficient with condensate saturation.

Introduction

During the exploitation of gas-condensate reservoirs, the bottom hole flowing pressure decreases gradually. Below the dew point pressure, retrograde condensation occurs leading to the segregation and then to the mobilization of the condensate phase (above the critical condensate saturation S_{cc}) towards the producing wells. The liquid phase accumulates in the wellbore region, forming a ring which impairs progressively the gas deliverability. In addition to that, steadily, the produced gas becomes lighter and therefore less marketable. Predicting reservoir gas performance and economy thus requires an accurate modeling of the flow behavior and the thermodynamics of those processes.

In the reservoir, far from the wellbore, flow rates are low and Darcy's law remains valid. It is possible to reproduce in the laboratory such flow rates and to study the fluid behavior. Some authors¹⁻⁵ studied the evolution of the critical condensate saturation with the gas-liquid interfacial tension (IFT). They measured gas and condensate relative permeabilities and correlated them with a capillary number. But near the wellbore, high pressure gradient induces both large condensate saturation and high gas velocities which may lead to significant deviations from Darcy's law for gas permeability. The near wellbore region plays a key role in the productivity decline of the field, and at the present time, no physically relevant model exists which takes into account these non-Darcian two-phase flow effects. A better description of flowing properties may lead to a better prediction of the productivity decline.

Background :

Much research has been conducted to understand the failure of Darcy's law when gas flow rate is gradually increased⁶⁻¹⁰. In 1914, Forchheimer⁶ proposed the following equation, which is still the most commonly used flow equation :

$$-\tilde{N}P = \mu/k.v + \beta r.v^2 \quad (1)$$

μ/k is the viscous Darcy's term and β is called inertial coefficient.

- Noman et al.⁴, Kalaydjian et al.³ summarized the origin of inertial effects and the influence of fluids and pore structure on β .

- In the case of an immobile liquid saturation, many correlations like Geertsma's one¹¹ exist, which express β as a function of porosity, permeability and gas saturation:

$$b \sim 1/(k^{0.5} . F^{5.5} . Sg^{5.5}) \quad (2)$$

- Inertial effects appear to be stronger for a gas phase flowing at high flow rates in a porous medium in the presence of a mobile liquid rather than a non mobile one¹². But this has never been supported by any conclusive experiment and no reliable correlation still exists.

- For gas-condensate flow, Coles and Hartman¹³ developed a method to estimate the effective β -coefficient at different liquid saturations : they use core samples containing various saturations of solidified paraffin wax that mimic an immobile condensate phase. But experiments were performed under ambient conditions. In addition, at high liquid saturation, above the critical liquid saturation, immobile paraffin is not representative of mobile liquid. Consequently, to take into account inertial effects, the Forchheimer equation is generally implemented in reservoir simulators with a $\beta(k, \phi, Sg)$ -correlation established for immobile liquid saturation. But neither the mobility of the liquid nor the thermodynamic conditions are considered. In the case of a gas-condensate field, this leads to a large inaccuracy in the prediction of well productivity.

Inertial effects under reservoir conditions have never been experimentally studied. For gas-condensate fields, only pioneering numerical simulation works were performed by Gondouin et al.¹⁴. Acquiring such laboratory data is important to establish and validate any correlation.

This paper presents a contribution to the improvement of the description of gas-condensate flowing properties in the near-wellbore region. Specialized laboratory equipment has been built at IFP in order to perform high velocity gas-condensate displacements, as representative as possible of near wellbore conditions.

With this equipment, a methodology was developed to measure the effective β -coefficient for gas and gas-condensate displacements.

The laboratory study was conducted with the aims :

- (i) to estimate the influence of the pore structure on the gas inertial coefficient, β , and
- (ii) to integrate the effect of the condensate dropout in the Forchheimer flow equation.

Experiments performed with consolidated and unconsolidated porous media and with analog gas-condensate systems are reported and the results are discussed.

Equipment and procedures

Apparatus :

It is quite difficult to model, in the laboratory, wellbore flow conditions, under pressure and temperature. Typically, for a production flow rate $Q_{\text{field}}(7\text{MPa};37.8^\circ\text{C})$ of $10^6\text{m}^3/\text{day}$, when using a C1-C3 binary fluid as an analog of a real gas-condensate system, this leads to operate in the laboratory 111 liters per hour³.

In order to reach such high flow rates under pressure and temperature and to simulate the wellbore flow conditions the prototype "Pegase" has been developed at IFP (Figure 1). Its main specifications are:

- (1) the capability to inject a large volume of fluid in the porous medium at fixed pressure drop ($\Delta P_{\text{max}}=20\text{bar}$), by means of two high flow rate pumps,
- (2) a good pressure regulation and an accurate control of flow rates.

The device includes two pumps, each equipped with one single cylinder of large capacity (15l). They can reach a flow rate of 100 liters per hour under 200 bar. The pump cylinders, the porous media and the different pressure transducers are all set in a temperature controlled airbath. During the experiments, pressures and temperature are automatically regulated and all the flow parameters are recorded by the central unit. For consolidated samples, the core is set into a horizontal Hassler-type cell, with an overburden pressure (isopar oil) 40 bar higher than the pore pressure. For the slim tube experiments, glass beads are compacted into standard tubes of 6 mm diameter.

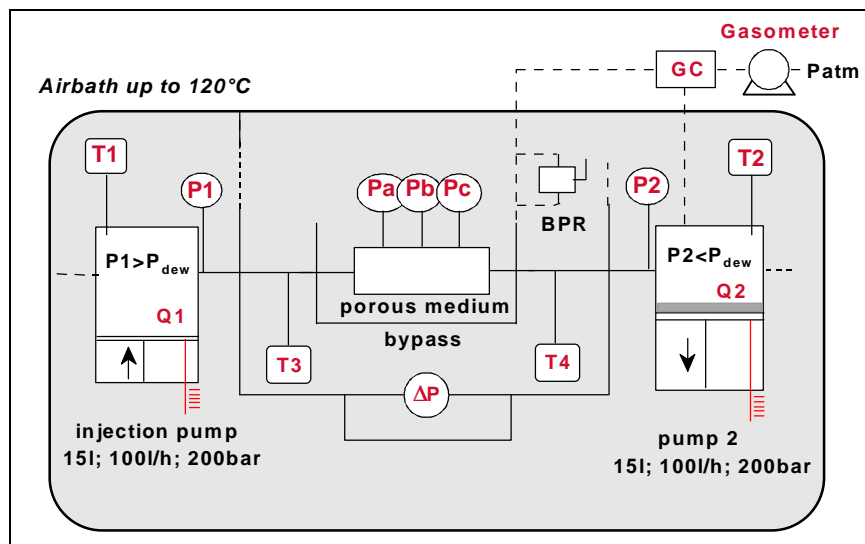


Figure 1 : PEGASE prototype

Measurement of β - Case of an immobile constant liquid saturation :

The objective is to study the influence of pore structure (k , ϕ , S_{wi}) on inertial effects in gaseous conditions. To measure the β -g-coefficient of various porous media, the following steps were performed :

- Initially, all the system (pumps and porous medium) is saturated with gas at a given pressure P_1 ($P_1=90\text{bar}$ for instance).
- The outlet pressure is reduced step by step down to selected values $P_2(i)= P_1- \Delta P(i)$, while the pump 1 injects continuously gas in the porous medium, at the constant pressure P_1 : Step (i) : at each pressure step (i), the inlet and outlet flow rates adjust themselves. Once the equilibrium is reached, that is once the flow parameters are stable, flow rates $Q_1(i)$ and $Q_2(i)$, pressures P_1 and $P_2(i)$ and differential pressure $\Delta P(i)$ are recorded and the outlet pressure is automatically reduced down to the next step value $P_2(i+1)$.
- The curves ∇P_1 vs. Q_1 and ∇P_2 vs. Q_2 can be drawn with the equilibrium values and the deviation of Darcy's law should be observed (Figure 2).
- β is deduced while plotting the pressure squared difference over the mass flow rate versus the mass flow rate Q_m ($Q_m=\rho.Q$). The slope of the curve gives β and the extrapolation of the ratio for $Q_m=0$ gives the effective permeability k (Figure 3).

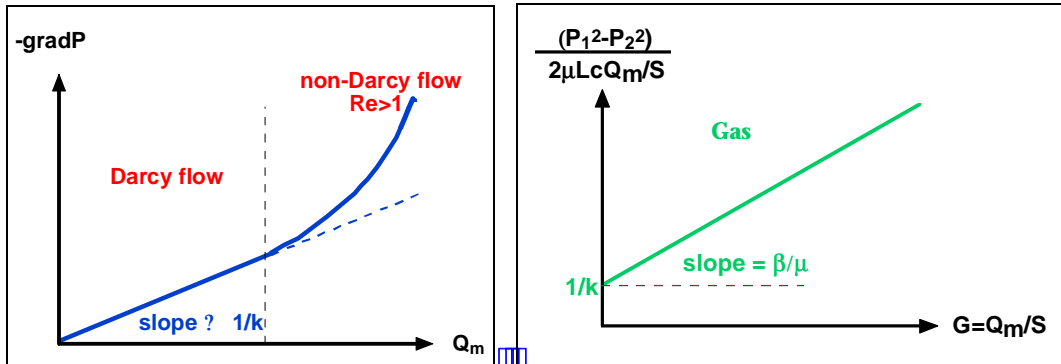


Figure 2 : Deviation of Darcy's law Figure 3 : Evaluation of β g coefficient

Remark : the integration of the Forchheimer equation $(P_1^2 - P_2^2)/(2\mu L c Q_m / S) = 1/k + \beta/\mu \cdot Q_m / S$ with $c=ZRT/M$ supposes that the variations of Z (compressibility) and μ (viscosity) between P_1 and P_2 are small enough to be considered as negligible.

For nitrogen, between 90 and 70 bar, the viscosity μ and the compressibility factor Z do not vary drastically and this integration can be applied (Table 1).

Pressure (bar)	μ (cP)	Z	density (kg/m^3)
1	0.0176	0.9998	1.15
5	0.0176	0.9989	5.74
10	0.0177	0.9979	11.49

70	0.0189	0.9953	80.66
80	0.0191	0.9966	92.06
90	0.0194	0.9985	103.37

Table 1 : Nitrogen properties at 21°C

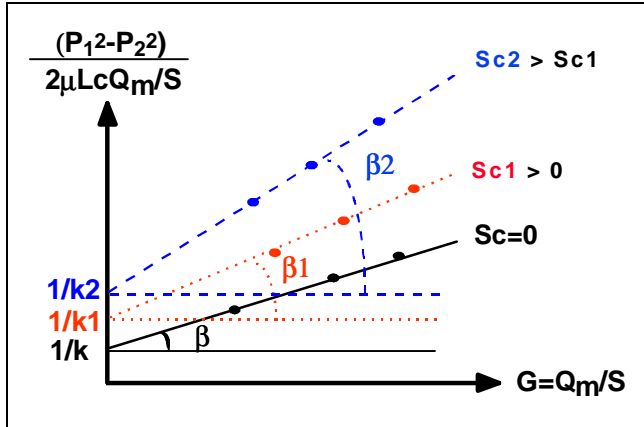


Figure 4 : Measurement of $\beta(Sc)$

Measurement of β - Gas-condensate case :

- Objective :

The objective is to study the influence of the condensate saturation on the β coefficient, that is to draw the Forchheimer curves $d(P^2)/P_1 Q_1$ vs. Q_m at various condensate saturations Sc (Figure 4).

- Principle of one experiment :

A well known C1-C3 mixture is considered at constant temperature.

1. Initially, the porous medium is saturated with gas in presence of connate water saturation. The pore pressure is above the dew point pressure P_d ($P_1 = P_2 > P_d$).

2. Pressure step (i) : the fluid is injected in the porous medium at a constant pressure P_1 slightly above P_d , while the outlet pressure is regulated at a constant selected value $P_2(i)$ below the dew point. In the porous medium, near the inlet, pressure becomes lower than P_d and condensate appears. This liquid accumulates and above the critical saturation Sc_c , it starts being mobile. Once pressures and flow rates are stabilized, they are measured. Figure 5a shows the shape of pressure and condensate saturation profiles obtained at this "dynamic" equilibrium. If P_1 is not far from P_d ($P_1 - P_d < 1 \text{ bar}$), 1D-simulations show that local ($Sc(i,x)$) and average ($Sc(i)$) condensate saturations are very narrow (1-2%) .

3. $Sc(i)$ measurement : when the "dynamic" equilibrium is reached, the porous medium is isolated. The pore pressure stabilizes to the average pressure $P_a(i)$ and a new saturation profile is obtained (Figure 5b). The average condensate saturation corresponding to this "static" equilibrium, $Sc(P_a(i))$, is deduced from material balance made during a miscible injection of C1 with effluent GC analysis. 1D-simulations show that this saturation and the average saturation $Sc(i)$ of the "dynamic" equilibrium are comparable (2-5%).

Steps 2 and 3 are repeated for different values of $P_2(i)$ and β -coefficient will be correlated with the average condensate saturation $Sc(P_a(i))$.

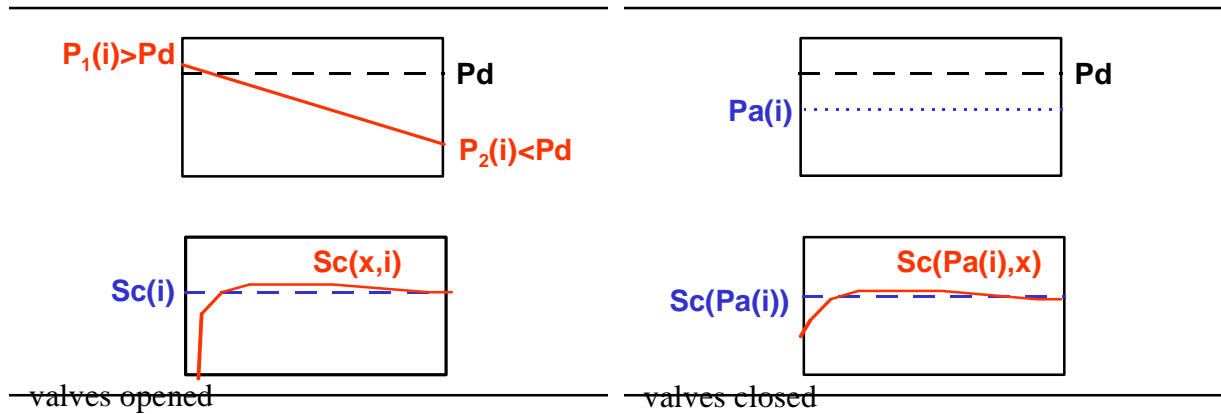


Figure 5a : P and Sc profiles at the "dynamic" equilibrium

Figure 5b : P and Sc profiles at the "static" equilibrium

- β measurement (Figure 6 and 7) :

β is a function of Sc . For its measurement (Figure 4), Sc should be fixed.

In a 4 step experiment with a given C1-C3 mixture, each step (i) corresponds to a pressure $P_2(i)$, to a condensate saturation $Sc(i)$. For each step (i) there is only one point in the Forchheimer diagram relative to $Sc(i)$ (Figure 6).

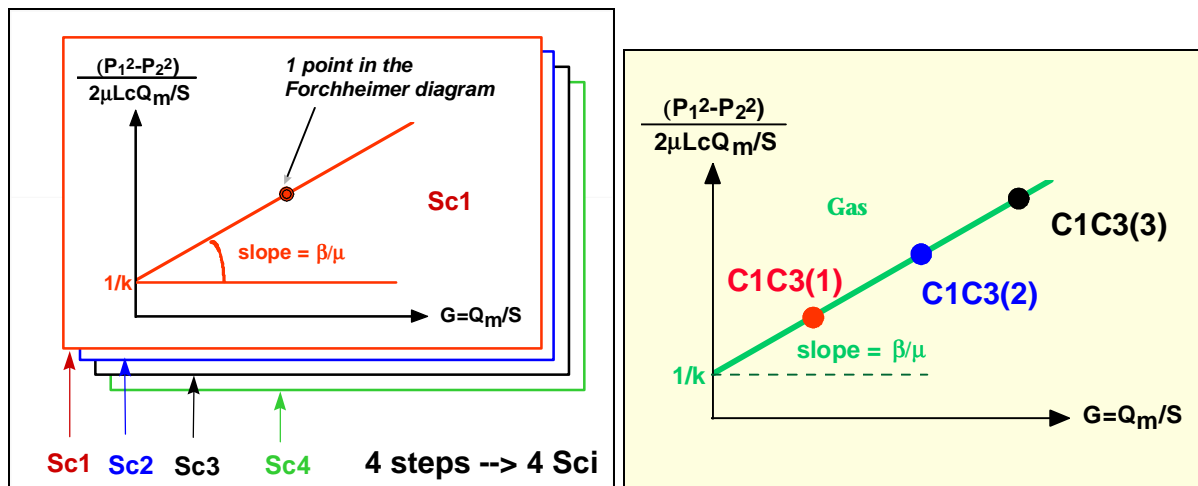


Figure 6 : 4 step experiment with one C1-C3 mixture

Figure 7 : Experiments with 3 C1-C3 mixtures - Sc fixed

For a given Sc , a minimum of three C1-C3 mixtures is needed to plot three points in the Forchheimer diagram (Figure 7). To reach a given Sc , the pressure conditions for each mixture have to be estimated. This conditions can be chosen by means of iterative simulations : after the experiment with a first fluid (first point in the Forchheimer diagram), the displacement of the second C1-C3 mixture is simulated with IFP numerical simulator ATHOSTM and an average saturation is calculated. The pressure conditions are then modified in order to obtain the same Sc as for the first fluid. The experiment performed at these calculated pressures will give a second point in the Forchheimer diagram. The same operation is performed for the third fluid

to obtain a third point in the Forchheimer diagram (Figure 7).

Results and discussion :

Porous media :

- Two sandstone core samples were selected from CT scan examination : Vosges sandstone (V4-2B : medium permeability) and Birchover sandstone (B1B : low permeability). Gas (Nitrogen) and brine (30g/l KCl) permeabilities were measured. Some experiments were performed at connate water saturation, S_{wi} . To establish S_{wi} , brine was first displaced by viscous oil. This was followed by successive floods of light oil, methane and finally nitrogen. The brine saturation profiles were checked for uniformity (CT-scan analysis before and after displacements). No significant heterogeneity of profiles was detected.

- Experiments were also performed on two slim tubes, ST1 and ST2, filled with calibrated glass beads (diameter : 20-40 μ m).

Table 2 shows the dimensions and the main characteristics of these porous media.

Porous Medium	Length (cm)	Diameter (cm)	Porosity (%)	Pore Volume (cc)	kw (mD)	kN2 (mD)	*d50 (μm)
V4-2B	40	4.87	21.9	163.9	169	211	8
B1B	24.85	4.85	15.8	72.5	28	40	3.5
ST1	613.5	0.6	37.9	65.7	2430	2510	~49
ST2	1000	0.6	36.3	102.6	2710	2670	~50

Table 2 : Porous media

*d50 is the average pore diameter corresponding to 50% of non-wetting saturation (from mercury pore size distribution curve)

Fluids :

- The experiments in single phase conditions were performed with nitrogen and air (for slim tubes) at ambient temperature (cf. N2 properties in Table 1).

- Gas-condensate experiments : It has been shown that analog fluid systems can be used instead of real ones to measure gas-condensate flow parameters³. The main advantage of using analog fluid systems is that, contrary to actual fluid systems, with binary fluid systems like C1-C3 mixtures, the pressure and temperature to be applied are not too high. At 38°C, the dew point pressure is about 90 bar whatever the composition of the C1-C3 mixture may be.

Table 3 gives the composition and the Maximum Liquid Dropout at 38°C (MLDO) of the three C1-C3 mixtures selected for the study. Figure 8 shows that the interfacial tension of C1-C3 mixtures do not vary drastically with pressure between 80 and 90 bar at 38°C (0.02-0.09mN/m). The Constant Volume Depletion (CVD) curves were determined experimentally at 38°C (Figure 9) and were compared with the ones calculated with the IFP PVT-Simulator.

As shown in Table 3, PVT simulations overestimate the Maximum Liquid Dropout (MLDO). This effect is due to the fact that, at 38°C we are near the critical point (Figure 10). In this region, it is well known that PVT calculations are never very accurate and overestimate the liquid dropout. Furthermore, experimentally near the critical point, a small impurity can drastically modify the thermodynamic equilibrium.

Fluid	C1 %mol	C3 %mol.	experimental MLDO (%liq.)	calculated MLDO (%liq.)	experimental Pd (bara)	calculated Pd (bara)
F1	59	41	8.2	17.6	89.1	90.7
F2	56	44	~20	47.9	91	91.4
F3	54.5	45.5	31.4	70.6	91	90.5

Table 3 : C1-C3 mixtures and CVD parameters at 38°C

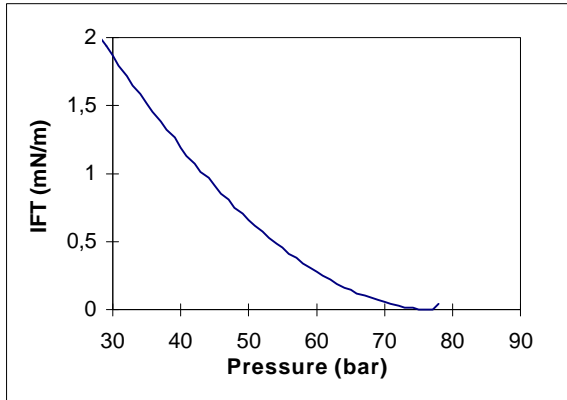


Figure 8 : IFT of C1-C3 mixtures at 38°C

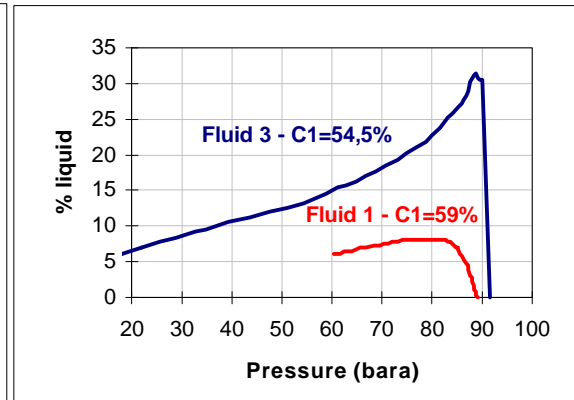


Figure 9 : Experimental CVD of fluids F1 and F3 at 38°C

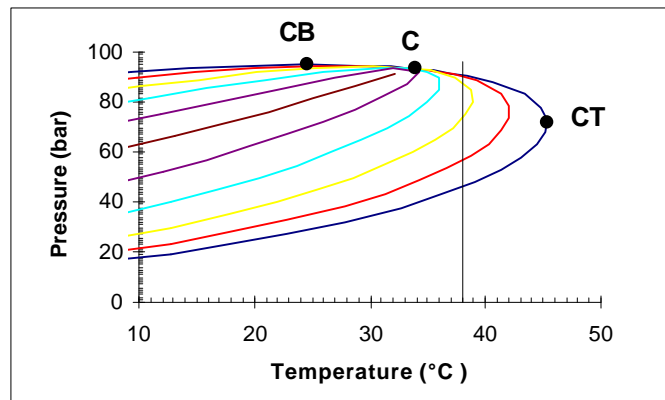


Figure 10 : Simulated phase envelope of fluid F1 (C1=59%mol.)

One phase flow experiments

The inertial gas coefficient was determined for the Vosges and Birchover sandstones and for the two slim tubes at various connate water saturations, following the above described procedure. Results are grouped in Table 4. Figure 11 shows a pressure cycle performed on the dry V4-2B sample. The measured flow rates and pressures show a deviation of Darcy's law. This deviation and the Forchheimer diagram used to estimate the β -coefficient are presented in Figure 12.

Comments :

- The measurements are reproducible (cf. Measurements on V4-2B at $S_{wi}=0.34$ - Table 4). In Table 4, measured β are compared with values calculated from Geertsma correlation :

$$\beta = 0.005 / (\phi^{5.5} \cdot k_w^{0.5}) \text{ (USI) for } Sw_i = 0 \quad (3)$$

$$\beta = 0.005 / (\phi^{5.5} \cdot (1 - Sw_i)^{5.5} \cdot k_g^{0.5}) \text{ (USI) for } Sw_i \neq 0 \text{ (with } k_g \text{ the effective permeability)} \quad (4)$$

The experimental values are quite different of the calculated ones. As observed in the literature, Geertsma correlation overestimates the inertial effects, particularly if water is present in the porous medium.

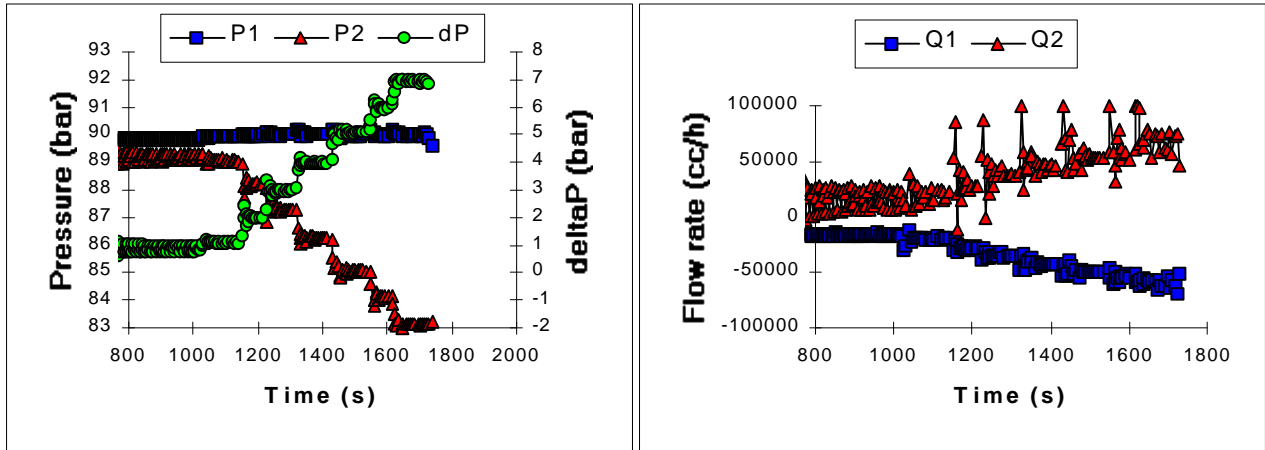


Figure 11 : β evaluation for V4-2B at $Sw_i = 0$ - Pressure cycle and flow rates

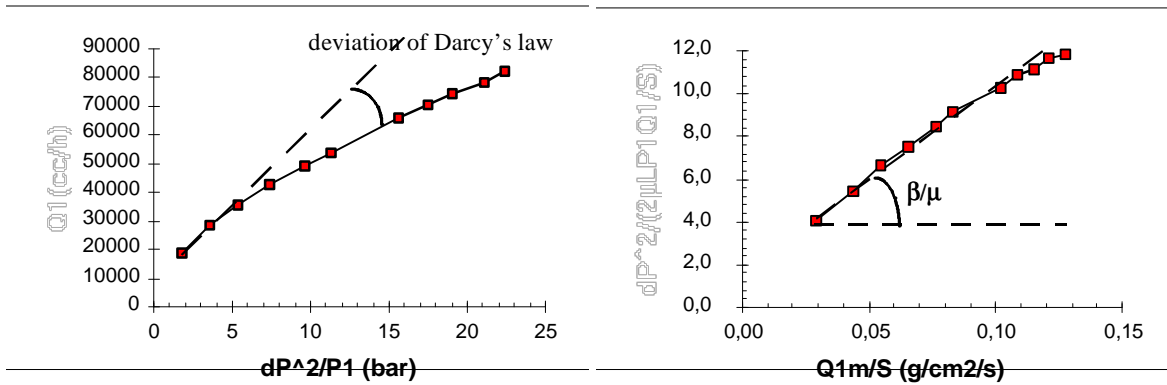


Figure 12 : V4-2B at $Sw_i = 0$: Deviation of Darcy's law and β measurement

Porous Medium	Swi (%PV)	Measured					Geertsma correlation			
		β (m^{-1})	β (ft^{-1})	ϕ	kw (D)	kg (D)	β (Swi=0) (m^{-1})	β (Swi>0) (m^{-1})	β (Swi=0) (ft^{-1})	β (Swi>0) (ft^{-1})
V4-2B	0	1.30E+08	3.96E+07	0.219	0.169	0.211	5.16E+07		1.57E+07	
V4-2B	34	1.92E+08	5.85E+07	0.219	-	0.208		4.57E+08		1.39E+08
V4-2B	34	1.90E+08	5.79E+07	0.219	-	0.208		4.57E+08		1.39E+08
V4-2B	40	2.80E+08	8.53E+07	0.219	-	0.096		1.14E+09		3.46E+08
B1B	0	1.12E+09	3.41E+08	0.158	0.028	0.04	7.63E+08		2.33E+08	
B1B	24.8	2.20E+09	6.71E+08	0.158	-	0.033		3.37E+09		1.03E+09

B1B	43	5.60E+09	1.71E+09	0.158	-	0.025		1.78E+10		5.42E+09
ST1 air	0	4.08E+05	1.24E+05	0.379	2.43	2.53	6.66E+05		2.03E+05	
ST1 N2	0	4.49E+05	1.37E+05	0.379	2.43	2.51	6.66E+05		2.03E+05	
ST1	18.3	5.74E+05	1.75E+05	0.379	-	2.02		2.22E+06		6.77E+05
ST2 air	0	4.11E+05	1.25E+05	0.363	2.71	2.69	8.00E+05		2.44E+05	
ST2 N2	0	4.02E+05	1.23E+05	0.363	2.71	2.67	8.00E+05		2.44E+05	

Table 4 : Measured and calculated inertial coefficients

Figure 13 shows an increase of β with the water saturation for both sandstones, as reported in the literature. The presence of water reduces the available pore volume and consequently porosity and permeability. It increases the number of direction changes and the flow path length of the fluid and consequently the pressure losses and β value.

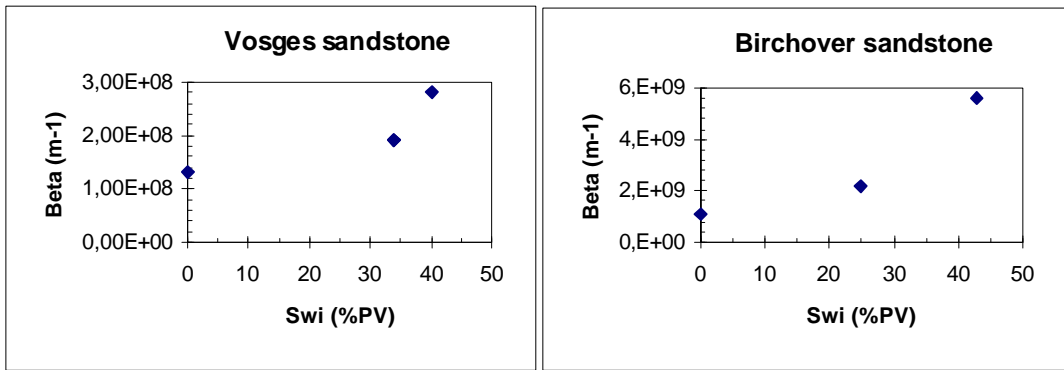


Figure 13 : Evolution of β with S_{wi}

In Figure 14 measured values have been compared to literature data¹⁵. They are in good agreement with previous published results. Figure 14 shows a decrease of inertial effects with the permeability as generally observed.

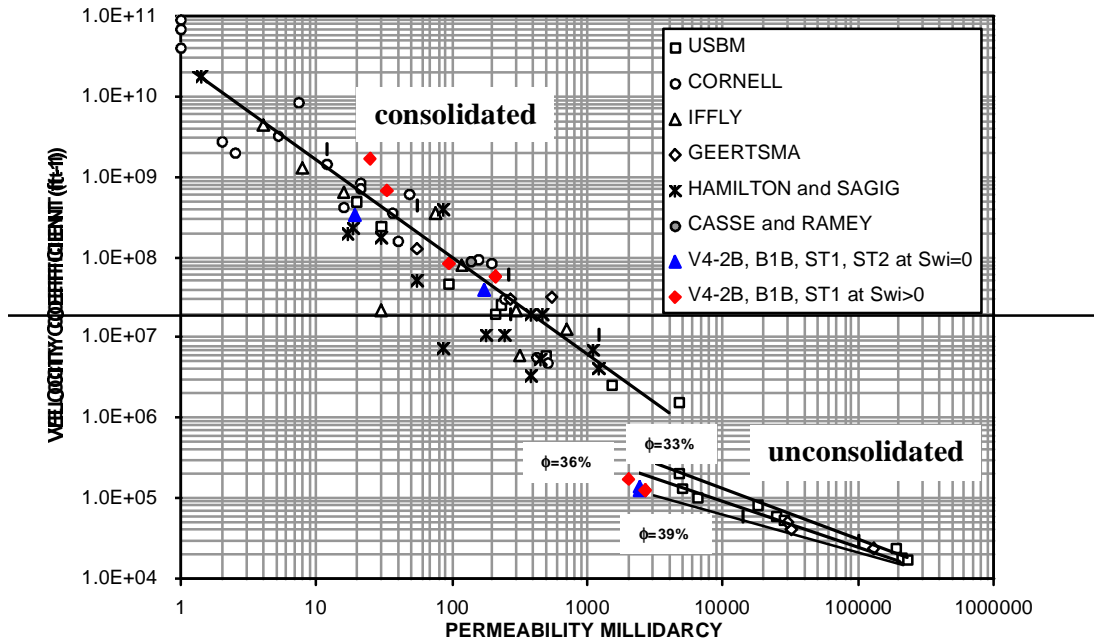


Figure 14 : Correlation of β with permeability¹⁵

An attempt was made to reconcile values obtained with and without S_{wi} . For each porous medium and each water saturation, an average equivalent pore radius, r^* , has been calculated with the following formula (Table 5) :

$$r^* = (8.k_w / \phi)^{0.5} \text{ (USI)} \quad \text{for } S_{wi}=0 \quad \text{or} \quad (5)$$

$$r^* = (8.k_g / \phi(1-S_{wi}))^{0.5} \text{ (USI)} \quad \text{for } S_{wi}>0 \quad (6)$$

These formula, established for bundles of identical capillaries from Poiseuille and Darcy's equations, leads to a good linear relationship : $\log \beta$ vs. r^* for all experiments (Figure 15). The inertial coefficient decreases as the equivalent pore radius increases, that is when the permeability increases or when the water saturation decreases.

PM	ϕ	S_{wi}	k_w (mD)	k_g (mD)	β (m ⁻¹)	r^* (μ m)
V4-2B	0.219	0	169	211	1.3E+08	2.48
V4-2B	0.219	0.34	-	208	1.9E+08	3.39
V4-2B	0.219	0.4	-	96	2.8E+08	2.42
B1B	0.158	0	28	40	1.1E+09	1.19
B1B	0.158	0.248	-	33	2.2E+09	1.49
B1B	0.158	0.43	-	25	5.6E+09	1.49
ST1	0.379	0	2430	2510	4.5E+05	7.16
ST1	0.379	0.185	-	2020	5.7E+05	7.23

ST2	0.363	0	2710	2670	4.0E+05	7.73
-----	-------	---	------	------	---------	------

Table 5 : Average pore radii and β

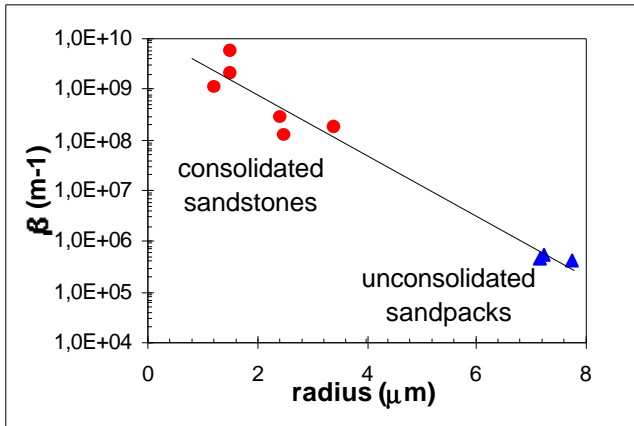


Figure 15 : Correlation β versus r^*

Gas-condensate high flow rate displacements :

Gas condensate displacements were performed in the Birchover sandstone (B1B at $S_{wi}=24.8\%PV$ - Table 2) with the C1-C3 mixtures given in Table 3 and following the above described procedure. For each fluid and each pressure step (i), the best regulation parameters (proportional bands of pumps) were selected in order to reach good equilibrium.

Figure 16 shows an example of experiment : Fluid 3 was injected in the B1B sample at constant pressure $P_1=89bar$ while pump 2 regulated the outlet pressure at $P_2=79bar$. The equilibrium, that is the stabilization of flow rates and pressures (equilibrium), was reached quickly (60s).

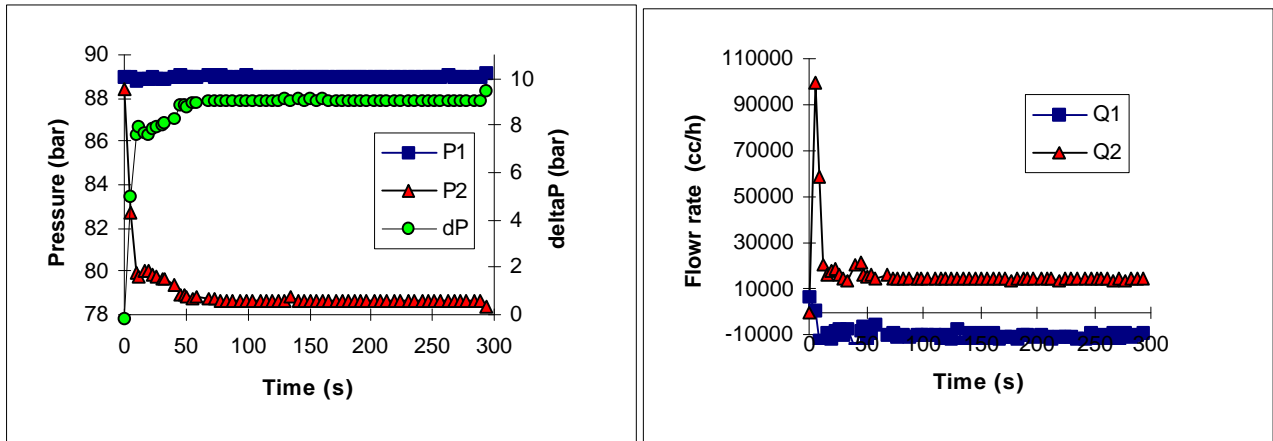


Figure 16 : B1B sample at $S_{wi}=24.8\%PV$ - Fluid 3 - Cycle $P_1=89bar$
 $P_2=79bar$ - $Sc=53.6\%PV$

The results of all the performed experiments are presented in Figure 17. On this Forchheimer diagram the error bars relative to the equilibrium flow rate measurements are reported for each point. Squares are relative to the measurement with the first fluid ($C1=59\%$) and the circles to the third fluid ($C1=54.5\%$). The measured condensate saturation is indicated for each point.

- As expected, all the points relative to a non zero condensate saturation are located above the reference line $Sc=0$ ($\beta=2.2 \cdot 10^9 m^{-1}$). The presence of condensate increases inertial effects.
- In Figure 17, it is difficult to interpret all the results in term of β -variation with Sc (as in

Figures 7 & 12). At a given Sc-value, it is not possible to find a linear correlation as for the gaseous case (Sc=0). For some experiments, the pressure and flow rate stabilization was bad, implying large error bars (C1=59% - Sc=0.47, 0.57, 0.75). The stabilization of the flow rate was really better for the rich fluid (C1=54.5% - circles in Figure 17). With this fluid the maximum condensate dropout is high, liquid appeared more rapidly in the porous medium, leading to high stable condensate saturation. Furthermore, the uncertainty on calculation of the average saturation is difficult to estimate : In addition to experimental inaccuracy, due to different thermodynamic conditions, the measured saturation $Sc(Pa(i))$ (Figure 5b : porous medium isolated, $P=Pa(i)$, no pressure gradient) may be slightly different of the saturation $Sc(i)$ (Figure 5a : "dynamic" equilibrium $P_1 > Pd > P_2$) at which pressures and flow rates were measured.

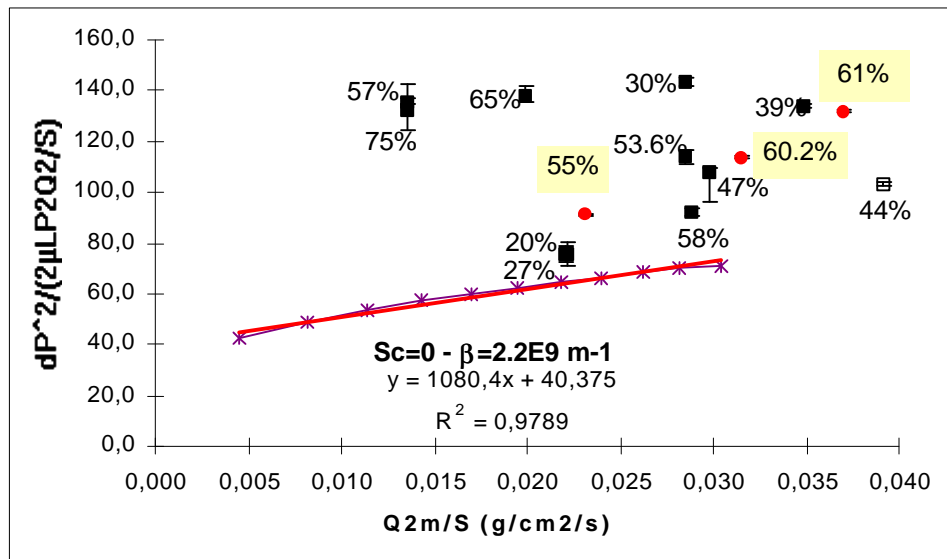


Figure 17 : Gas condensate displacements in B1B at $S_{wi}=24.8\%PV$ - Forchheimer diagram

- Interpretation attempt :

For some experiments, the measured values of the condensate saturation were quite narrow (Sc=55%PV, 58%PV, 60.2%PV, 61.0%PV). Considering that these experiments have been performed at the same condensate saturation (average value Sc=58.6%PV), it is possible to estimate a β -value. Figure 18 presents the Forchheimer diagram relative to Sc=58.6%PV. The slope of the curve leads to the coefficient $\beta(Sc=58.6\%PV)=5.6 \cdot 10^9 m^{-1}$ with a good correlation factor ($r^2=0.92$). This value is much higher than the one obtained at Sc=0

since it is increased by a factor 25.

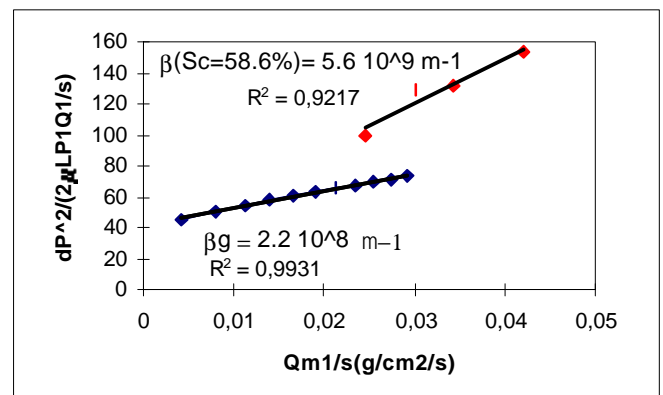


Figure 18 : β -value of B1B at

Swi=0.248 and Sc=0.586

Future work :

To establish $\beta(S_c)$ correlations, other experiments have to be performed, at different condensate saturation values, with other fluids. To reduce the uncertainty on the equilibrium flow rates it would be better to work with rich fluids. Furthermore Figure 10 showed that at 38°C, a C1-C3 mixture is near the critical point. This temperature is only 3.5°C higher than the critical temperature of Fluid 3. In this region, the thermodynamic properties are difficult to calculate and experimentally, the equilibrium is very sensitive to any impurity. To avoid these problems and to work far from the critical point, C1-C4 mixtures could be used : actually, calculations show that a working temperature of 60°C is respectively 6.5°C and 45.5°C higher than the critical temperature of C1-C4 mixtures with a composition of C1=70% and C1=80%. The calculated CVD curves of these C1-C4 mixtures at 60°C give liquid dropouts in the range 2-25%.

Conclusions :

In order to improve the description of gas-condensate flowing properties in the near-wellbore region, a specific laboratory equipment has been built at IFP. This prototype, « Pegase », can simulate the pressure, temperature and high flow rate (1.5cm/s) conditions occurring near the wellbore. With this equipment, a methodology is proposed to measure the effective inertial coefficient of Forchheimer equation, β , for gas and gas-condensate displacements.

The inertial coefficient was measured for consolidated sandstones (Vosges and Birchover) and unconsolidated sandpacks (slim tubes) in gaseous conditions at various water saturations (immobile). The results are in good agreement with literature data.

- Measurements are reproducible ;
- β is higher for consolidated porous media than for unconsolidated porous media ;
- β increases as the permeability decreases ;
- β increases with the water saturation [for the Birchover sandstone, that is for the less permeable sample, $\beta(S_{wi}=0.43) = 5.\beta(S_w=0)$] ;
- β is well correlated and decreases with the average pore radius, r^* .

The study of the effect of the condensate dropout on β was started with the Birchover sandstone at $S_{wi}=24.8\%PV$. C1-C3 mixtures were used as analog gas condensate systems. The performed experiments showed that the presence of condensate increases inertial effects. β was estimated for an average condensate saturation of 58.7%PV with the most accurate measured flow rates. $\beta(S_c=58.7\%PV)$ was found to be significantly higher than the value measured at zero condensate saturation (factor 25).

To establish a $\beta(S_c)$ correlation, other experiments have to be performed, at different condensate saturation values. Performing experiments with C1-C3 mixtures leads to work near critical conditions, for which calculations and experiments are not very accurate. In order to avoid working under those conditions, future work will be devoted to C1-C4 high flow rate displacements.

Nomenclature

C1-C3=methane-propane
d = core diameter, m
d50 = average pore diameter, m
IFT = interfacial tension, mN/m
k = absolute permeability, m²
kg = effective gas permeability, m²
L= core length, m
M = molar weight, g/mole
MLDO=Max. Liquid Dropout, % liquid volume
P = pressure, bar
Pa = average pore pressure, bar
Pd = dew point pressure, bar
Pc= critical pressure, bar
PV= pore volume, m³
Q = flow rate, m³/s
Qm = mass flow rate, kg/s
r*= average equivalent pore radius, m
S = core section, m²
Sc= condensate saturation, %PV
Scc= critical condensate saturation, %PV
Sg = gas saturation, %PV
Swi= connate water saturation, %PV

T = temperature, °C
Tc= critical temperature, °C
USI = SI Units
v = velocity, m/s
Z= compressibility factor
β = inertial coefficient, m⁻¹
ΔP = differential pressure, bar
φ = porosity, fraction
ρ = density, g/cm³
μ = viscosity, cP

Subscripts

1 = inlet
2 = outlet
amb = ambient
c = critical
g = gas (vapor) phase
(i) = pressure step
i = irreducible
N2 = Nitrogen
w = water
wb = wellbore
res = reservoir

Acknowledgments

This research program has been partly funded by an industrial consortium involving AGIP, Gaz de France, Sonatrach and Total. We wish to acknowledge the members of this consortium for their permission to publish these results, for their valuable discussions and insights which contributed to the completion of the work.

References

1. Henderson, G.D., Danesh, A., Tehrani, D.H., and Peden, J.M.: "An Investigation into the Processes Governing Flow and Recovery in Different Flow Regimes present in Gas-Condensate Reservoirs," paper SPE 26661 presented at the 1993 SPE Annual Technical Conference and Exhibition, Houston, TX, Oct. 3-6.
2. Henderson, G.D., Danesh, A., Tehrani, D.H., Al-Shaidi, S., and Peden, J.M.: "Measurement and Correlation of Gas Condensate Relative Permeability by the Steady-State Method," paper SPE 30770 presented at the 1995 SPE Annual Technical Conference and Exhibition, Dallas, TX, Oct. 22-25.
3. Kalaydjian, F. J-M., Bourbiaux, B.J., and Lombard, J-M. : "Predicting gas-condensate reservoir performance : how flow parameters are altered when approaching production wells," paper SPE 36715 presented at the 1996 SPE Annual Technical Conference and Exhibition, Denver, Colorado, Oct. 6-9.
4. Noman, R., and Archer, J.S.: "The Effect of Pore Structure on non-Darcy Gas Flow in some Low-permeability Reservoir Rocks," paper SPE/DOE 16400 presented at the 1987 SPE/DOE Low Permeability Res. Symposium, Denver, May 18-19.
5. Gravier, J.F., Lemouzy, P., Barroux, C. and Abed, A.F.: "Determination of Gas-Condensate Relative Permeability on Whole Cores Under Reservoir Conditions," *SPE FE* (February 1986), 9-15.

6. Forchheimer, P.: "Wasserbewegung durch Boden," *Zeit. Ver. Deutsh. Ing.*, 1901, 45, 1781-1788.
7. Fancher, G.H., and Lewis, J.A.: "Flow of Simple Fluids through Porous Materials," *Ind. Eng. Chem.*, 1921, 25, 1139-47.
8. Cornell, D., and Katz, D.L.: "Flow of Gases through Consolidated Porous Media," *Ind. Eng. Chem.* (Oct., 1953) 2145-2153.
9. Tek, M.R.: "Development of a Generalized Darcy Equation," *Trans. AIME*, 1957, 210, 376.
10. Tek, M.R., Coats, K.H., and Katz, D.L.: "The Effect of Turbulence on Flow of Natural Gas through Porous Reservoir," *J. Pet. Tech.* (July, 1962) 799-806.
11. Geertsma, J.: "Estimating the Coefficient of Inertial Resistance through Consolidated Porous Media," *SPE J* (October, 1974) 445-450.
12. Wong, S.W.: "Effect of Liquid Saturation on Turbulence Factors for Gas Liquid Systems," *J. Can. Pet. Tech.* (Oct.-Dec., 1970) 274-278.
13. Coles, M.E., and Hartman, K.J.: "Effect of Liquid Saturation on Turbulence Factors for Gas Liquid Systems." "Non-Darcy measurements in dry core and effect of immobile liquid," SPE Gas Technology Symposium, Calgary, Alberta, March 15-18, 1998.
14. Gondouin, M., Iffly, R., and Husson, J.: "An Attempt to Predict the Time Dependence of Well Deliverability in Gas Condensate Fields," *SPE J* (June 1967) 113-124.
15. Firoozabadi, A., and Katz, D.L.: "An Analysis of High Velocity Gas Flow through Porous Media," *J. Pet. Tech.*, 1979, Feb., 211-215.